The Influence of Source and Matrix Nonuniformity on the TMU and Bias of Large Container Gamma-Ray Assay Results

Brian M. Young, Stephen Croft, and Hank Zhu
Canberra Industries, Inc., 800 Research Parkway, Meriden CT 06450, USA

Abstract
In the gamma-ray assay of containers such as 200 liter drums and large crates, several factors can contribute significantly to the total measurement uncertainty (TMU) and even give rise to a bias in the reported activity. A major contributor, and in many cases the leading contributor, in this arena is the nonuniformity of the distributions of activity and attenuating matrix within the container. This is because, lacking detailed information about these distributions, the assay of a given container is generally based around the assumption of uniformity. Differences between the uniform assumption and the actual distribution within a particular container can have very large effects on the final assay result depending on the energy of interest and the matrix density and degree of heterogeneity. A specialized Monte Carlo technique has been developed to model random spatial distributions of both source and matrix within typical containers and has been used to map out distributions of assay results (i.e. ratio of measured result to true activity) over a range of container types, gamma-ray energies, sample densities, and degrees of nonuniformity. These results will be presented along with simple semi-empirical formulae which parameterize these contributions to assay TMU and bias for common assay situations.

Introduction

A common gamma-ray measurement scenario is the radioassay of potentially active or contaminated material in large containers. Common containers include the familiar 200 liter drum and B-25 boxes. Within the U.S. Department of Energy community, the Standard Large Box 2 (SLB2, approx. 7000 liters) and the Standard Waste Box (SWB, approx 2000 liters) also find frequent use. For purposes of screening and free release, two competing objectives in the design of any gamma-ray assay system are high throughput and high sensitivity. A typical strategy for meeting both objectives is to assay the container from many detector positions so as to ensure that the entire sample volume is "seen" by at least one detector. Typically multiple detectors acquire data concurrently.

An example implementation of such a strategy is the Canberra WM-2500 Series Box Counter. In this system, four high-purity germanium (HPGe) detectors are used to assay the sample container. Two detectors are stacked vertically on either side of the container, which moves on a trolley between the two detector assemblies. The assay takes place with the trolley and sample located at multiple stationary positions along its length. So if a large box such as an SLB2 is assayed, for example, with five trolley positions, and with four detectors counting at each position, there are thus 20 detector locations which comprise the assay dataset. This is depicted in Figure 1.

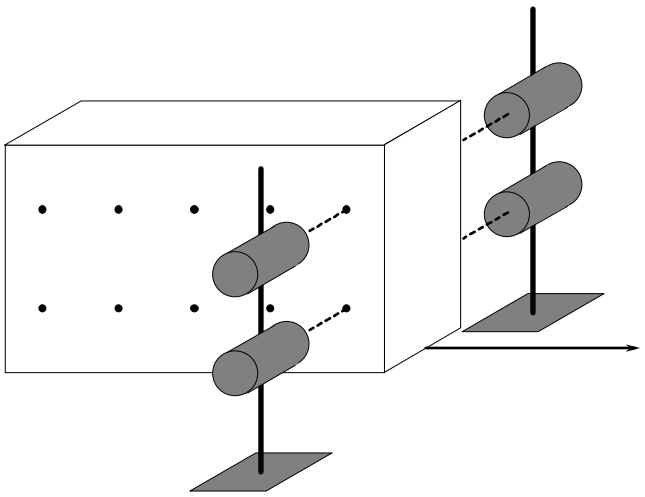

Figure 1. Illustration of typical Box Counter geometry.

For multi-position assays such as this, the most sensitive measurement result, that is the one with the lowest detection limit, is generally obtained from analyzing the summed spectrum from all of the detector locations. In order to obtain activity values from the accumulated spectrum, an efficiency calibration (i.e. full-energy-peak counts registered in the spectrum per gamma ray emitted in the sample medium) must be used. Typically the efficiency used during data analysis is obtained assuming that both the activity and the attenuating sample matrix are uniformly distributed throughout the volume of the container. This is in spite of the well-known fact that such uniformity is very rarely realized with actual sample waste containers. There are several reasons for nevertheless making the assumption of uniformity. One common reason is simplicity of calibration – whether one calibrates via measurement of prepared surrogates or via mathematical calculations, it's often cheaper, faster, and easier to use a uniform source term. Another, more important, reason is that if a large number of containers is to be counted, each with its own unknown degree and configuration of nonuniformity, the only reasonable assumption one *can* make is that of uniformity. Note that this does assume random packing and filling for each individual container; such an assumption is frequently justified. However, for a given container the difference between the actual (and usually unknown) source and matrix configuration and the uniformity that is assumed in the efficiency calibration can have significant impact on the accuracy of the final assay result.

The origin of these effects can easily be seen by examining a general expression for the summed efficiency for several detectors counting a container volume with arbitrary distributions of activity and attenuating matrix.

$$\varepsilon = \frac{1}{A_{Total}} \sum_{\text{Detectors}} \int_{\text{Container}} A(\vec{r}) \cdot \frac{e^{-\mu(\vec{r}) \cdot x(\vec{r})}}{d(\vec{r})^2} \cdot F(\theta_{\vec{r}}) \cdot dV$$

In this expression, each differential volume unit dV has an activity concentration A and thus is treated as a point source in the above equation. A line of sight exists between the point source dV and each detector. This vector has a total length d, and passes through attenuating materials μ over path-length x on its way out of the container. The function F represents the angular response

of each detector for off-axis point sources. In the above equation, nearly every quantity in the integrand is labeled with the notation $\vec{r}$ to emphasize its dependence on position within the container volume. Nonuniformities enter the calculation explicitly in two places – the activity distribution within the sample volume is represented by the quantity $A(\vec{r})$, and the distribution of attenuating matrix is represented by the combined quantity $\mu(\vec{r}) \cdot x(\vec{r})$. Note that the quantity $\mu(\vec{r})$ and to a lesser degree $F(\theta_{\vec{r}})$ are both energy dependent. The uniform case, which is assumed during efficiency calibration, is obtained by making both $A(\vec{r})$ and $\mu(\vec{r})$ constants, independent of position within the sample volume.

For any given, generally nonuniform, container, the efficiency can be represented by the quantity $\varepsilon_{\text{Nonuniform}}$. The uniform efficiency, assumed for calibration, can be represented by the quantity $\varepsilon_{\text{Unif., Calib.}}$. Thus, when the container is assayed, the ratio of the measured activity to the true activity is given by the ratio $R = \dfrac{\varepsilon_{\text{Nonuniform}}}{\varepsilon_{\text{Unif., Calib.}}}$. If the sample container is indeed uniform – in other words if the sample geometry matches the calibration geometry – then the ratio is unity. It is also easy to see that substantial discrepancies can also arise. If the activity exists as a single concentration buried deep in the container, then few (or no) gamma rays may survive unattenuated to the detectors, and the measured activity will be lower than the true activity. Alternatively, if the activity is concentrated on the periphery of the container, shining brightly into the detectors, then the measured activity will be higher than the true activity. One can quantify these extreme limits rather simply by hand or via physics software such as MCNP™ [1] or Canberra's ISOCS [2]. However, this approach requires individual calculation of each nonuniform geometry and is thus useful primarily for examining the extreme cases. More generally one would like to examine the probability distribution of ratios for a large population of nonuniform cases. From this distribution it is possible to examine such quantities as the population average, the most likely ratio, and confidence bounds.

Monte Carlo Technique

To facilitate this sort of examination, a dedicated Monte Carlo technique has been developed to explore the distribution of *R* values for point activities randomly distributed inside randomly-configured sample matrices. The technique is implemented in ANSI C code and compiled to run under Windows XP. The primary input required by the code consists of the dimensions of the container and the (*x*,*y*,*z*) coordinates of the various detector locations, and the number (*N*) of point sources assumed to be randomly positioned within the container volume.

Attenuating materials, both in the sample matrix and in the container walls themselves, are specified by attenuation coefficient values μ expressed in units of cm^{-1}. Note that this encompasses three physical aspects of the measurement problem. First, a photon energy is chosen for the problem (e.g. 662 keV from ^{137}Cs); then a particular material is chosen, such as cellulose. From these two quantities, a mass attenuation coefficient $\left(\dfrac{\mu}{\rho}\right)$ expressed in units of $cm^2 \cdot g^{-1}$ is obtained from standard look-up tables. Finally a material density, in $g \cdot cm^{-3}$, is chosen for the material and multiplied by the mass attenuation coefficient to obtain the linear attenuation coefficient value used by the software. To specify a uniform sample matrix, then, a single

attenuation coefficient is sufficient. The software will also treat nonuniform matrices. To do this, it is necessary to specify a series of attenuation coefficients and volume fractions for the various materials that make up the overall sample; up to four such materials are allowed. So, for example, to specify a sample consisting of 80% cellulose and 20% void space the input would be the attenuation coefficients for cellulose and air with volume fractions of 0.8 and 0.2, respectively. The mechanism by which this information is used in the Monte Carlo calculations is described below. From the material specifications, the volume-average attenuation coefficient is calculated.

In the Monte Carlo model, the sample matrix is assumed to be divided into a 20 x 20 x 20 three-dimensional grid of volume elements (i.e. "voxels"). To set up a single random case, the 8000 voxels are randomly populated with attenuation coefficient values with the appropriate volume fractions (i.e. probabilities) from the information described above. Then, the specified number of point sources are randomly positioned inside the sample volume. The efficiency for this random configuration is then obtained by evaluating an expression that is explicitly parallel to the equation presented above in the Introduction. The physical model is depicted in Figure 2.

$$\varepsilon_{\text{Nonuniform}} = \frac{1}{\sum_{\text{Pt Src } i}^{N} A_i} \cdot \left(\sum_{\text{Pt Src } i}^{N} \sum_{\text{Pt Det } j} A_i \cdot \frac{e^{-\sum_{\text{Path } k(i,j)} \mu_k x_k}}{d_{ij}^2} \cdot F\left(\theta_{ij}\right) \right)$$

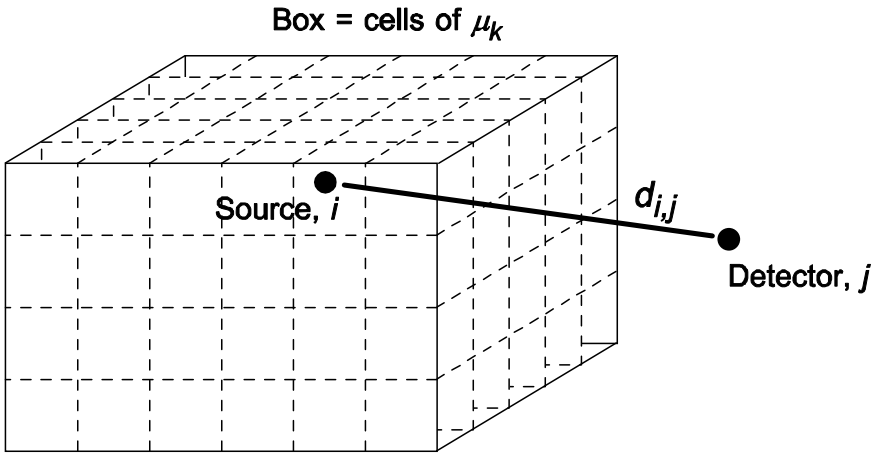

Figure 2. Illustration of model implemented in Monte Carlo software.

In this model, each point source is assumed to have the same activity *A*. The detectors are treated as point sensors that have unit intrinsic efficiency. The function $F\left(\theta_{ij}\right)$ allows for an angular dependence on the detector response. This allows for approximation of the intrinsic spatial dependence of the detector itself as well as the possible existence of a collimator. A few simple models have been implemented – a flat response versus angle, a step response versus angle, and a trapezoidal response versus angle.

To predict the assay ratio *R* for a given nonuniform case, it is necessary to calculate the uniform efficiency – this quantity is required for the denominator of the *R* ratios. To do this, the entire

sample volume is assigned the volume-average attenuation coefficient and the above expression is evaluated for "many" (typically 10^6-10^7) random point source locations. In effect, this evaluates the uniform volume integral. In other words, if one could homogenize the contents of a nonuniform container and use it to construct a surrogate for calibration, this would be the estimated calibration result. The uniform efficiency is evaluated once at the beginning of a run and then used in the denominator of *R* for all nonuniform test cases.

In summary, the flow of the software then goes as follows. First the input data are read and processed. The uniform efficiency $\varepsilon_{\text{Unif., Calib.}}$ is calculated using the volume-average attenuation coefficient for the sample volume and with many randomly distributed point sources. Then, to run a population of nonuniform cases, the following process is iterated – first the 20 x 20 x 20 sample grid is randomly populated with attenuation coefficient values as described above, then the *N* point sources are randomly positioned within the container, the above expression for $\varepsilon_{\text{Nonuniform}}$ is evaluated, and finally *R* is calculated. This process is iterated for typically 500,000 different random configurations, thereby building up a large population of assay ratios; that is, many more than could be explored experimentally.

Two versions of the code have been written. One version treats box containers and operates as already described. A second version treats cylindrical containers and operates the same way but with the following differences. The sample material grid is still Cartesian, but the cylindrical boundary of the container is now a circle superimposed on this grid in the *x*-*y* plane. Also, the possibility of a rotating container (e.g. a drum on a turntable) is treated by averaging over *n* discrete angular transformations. Typically, a value of 16 is used. The obvious value of $n = 1$ is used for the case where there is no rotation during the assay.

Results for Large Boxes – SLB2 Containers

A campaign of calculations was run for SLB2 containers. These boxes are roughly 165 cm x 165 cm x 265 cm with steel walls roughly 0.4 cm thick. Calculations were run for all combinations (42 in total) of the seven energies and six materials listed in Table 1.

Energy (keV)		Material, Density ($g \cdot cm^{-3}$)
59	(^{241}Am)	Air, 0.0012
129	(^{239}Pu)	Cellulose, 0.1
186	(^{235}U)	Cellulose, 0.4
414	(^{239}Pu)	Concrete, 0.7
662	(^{137}Cs)	Concrete, 1.0
1001	(^{238}U)	Concrete/Steel (0.8/0.2 vol.), 1.6
1333	(^{60}Co)	

Table 1. Summary of lines and materials modeled.

For each energy-material-density combination (i.e. for each μ value), 500,000 configurations were run assuming five point sources randomly placed within the container volume. The counting geometry was typical for a Canberra WM-2500 Series Box Counter – 20 detector positions (i.e. four detectors at five trolley positions along the length of the box) at a distance of roughly 60 cm from the sides of the box. The frequency (probability) distributions of the assay

ratios are presented in the Figure 3 for four representative material-density combinations at 662 keV.

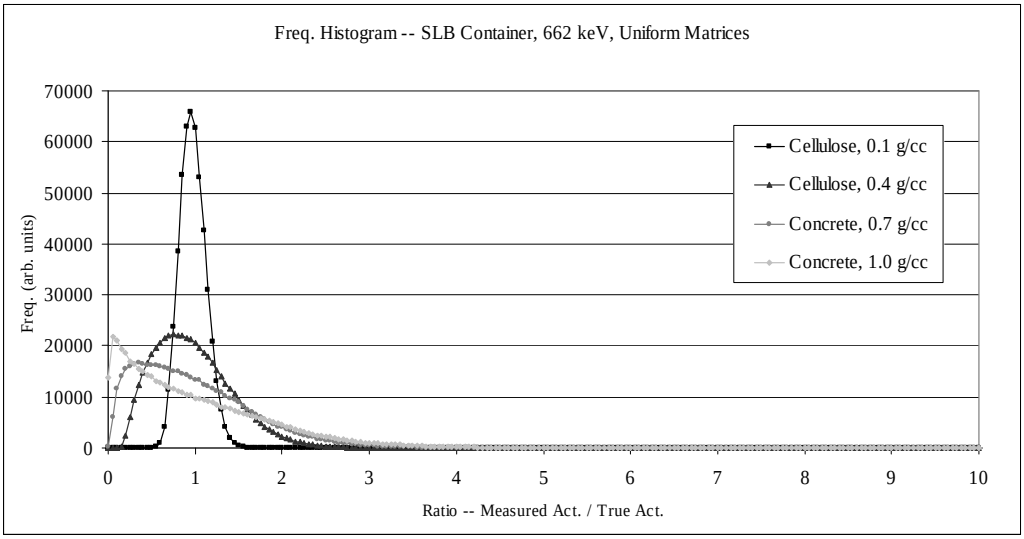

Figure 3. Frequency distribution of measured to true activity at 662 keV.

There are several features to discuss. Most obvious, for a relatively benign matrix (low atomic number (Z) material, low density), the distribution is fairly symmetric and centered about unity; and as the matrix becomes more challenging (higher-Z, higher density) the distributions become broader and more skewed towards low ratios (i.e. under-reporting of activity). In fact, for all but the most benign matrices, the *most probable* ratio is always less than unity. Although not immediately obvious from the above figure, for *each* energy-material-density combination, the *average* ratio is unity, as it should be. This underscores the assertion that if one assumes random packing and filling for each individual container, the optimum assumption for a waste stream at a given energy-material-density is uniformity.

One can take these distributions and estimate confidence bands. Since the distributions are generally asymmetric, it doesn't seem sensible to simply calculate a second moment of each distribution and report that as the "standard deviation". Instead it makes more sense to approach these distributions from a probabilistic standpoint. Specifically, $\pm 3\sigma$ bounds are commonly used as a starting point for estimating TMU values in Canberra's NDA2K software, implemented to handle multi-detector non-destructive assay systems. For a pure Gaussian distribution, the $\pm 3\sigma$ bounds encompass ~ 99.730% of the probability under the distribution; or alternatively ~ 0.135% of the probability lies outside the bounds in each direction. Understanding this, one can then look for similar probability bounds for the above (highly asymmetric) ratio distributions. Namely, one can define the probabilistic equivalent to "$\pm 3\sigma$" bounds as those that encompass 99.730% of the probability. These bounds have been determined from all of the cases run and are shown versus attenuation coefficient in Figure 4. "$\pm 1\sigma$" bounds are shown as well. For attenuation coefficient values below roughly 0.01 cm^{-1}, the $\pm 3\sigma$ boundaries flatten out to roughly ± 30%. This includes all of the empty box (i.e. air-filled) cases, which have attenuation coefficient values in the 10^{-5}-10^{-4} cm^{-1} range and are thus below the plotted range in the figure.

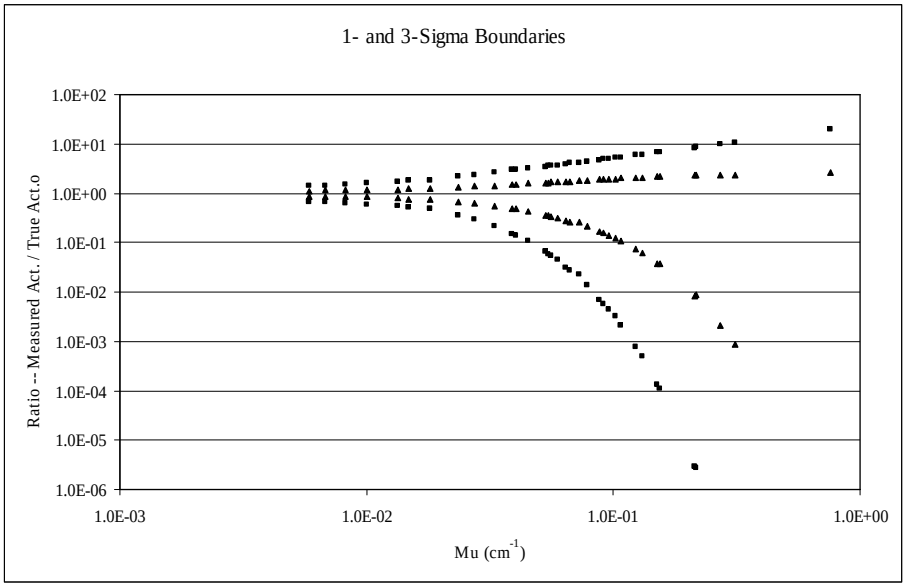

Figure 4. 1- and 3-sigma confidence limits for the SLB2.

Essentially, at such low attenuations, the ratio distributions are dominated by the $1/r^2$ behavior of the source-detector response. At higher attenuation values, the low-ratio boundary drops drastically. This is due to the potential for localized activity to become increasingly "buried" inside the container matrix. The high-ratio boundaries show a less dramatic effect. They are due to localized activity on the periphery of the container and are thus limited by geometry. Simply put, as the matrix gets more attenuating, it's always easier to push the sources "just a little deeper" whereas it's less easy to push the sources "just a little closer" to the edge of the container. It should be noted that most common assay situations dealing with containers as large as an SLB2 are restricted to attenuation coefficient values (i.e. energy-material-bulk density) ranging from 0.01 to 0.1 cm^{-1}. Over this range, the estimated 3σ TMU's equate to roughly a factor of 300 underestimate and roughly a factor of 8 overestimate for the highest attenuations.

One important aspect to note is that the boundary versus μ curves are well behaved. This makes it possible to map out the TMU boundaries at a few representative cases and use an interpolation scheme – a 3rd degree polynomial in log-log space appears to be adequate – to estimate the TMU boundaries at other arbitrary points at the time of assay.

Results for 200 Liter Drums

A similar campaign of measurements was run for rotating 200 liter drums. For each μ value, 500,000 configurations were run assuming three point sources randomly placed within the drum. As above, the counting geometry was typical for a WM-2500 Series Box Counter, with four detector positions (i.e. only one position, centering the detectors on the drum axis) at a distance of roughly 60 cm from the sides of the box. The frequency distributions show similar features to the ones presented above for the SLB2. Naturally, since the 200 liter drum is a smaller container, the distributions are not as drastically skewed as the ones above. Presented in Figure 5 are the 1σ and 3σ bounds calculated as before. At very low attenuation values, the 3σ bounds flatten out to roughly ± 5%. While the general shape and behavior of the curves is very similar to that for the

SLB2, the bounds aren't as large. When restricted to typical attenuation values between 0.01 and 0.1 cm^{-1}, the 3σ TMU's are estimated to be within factors of 3 to 5.

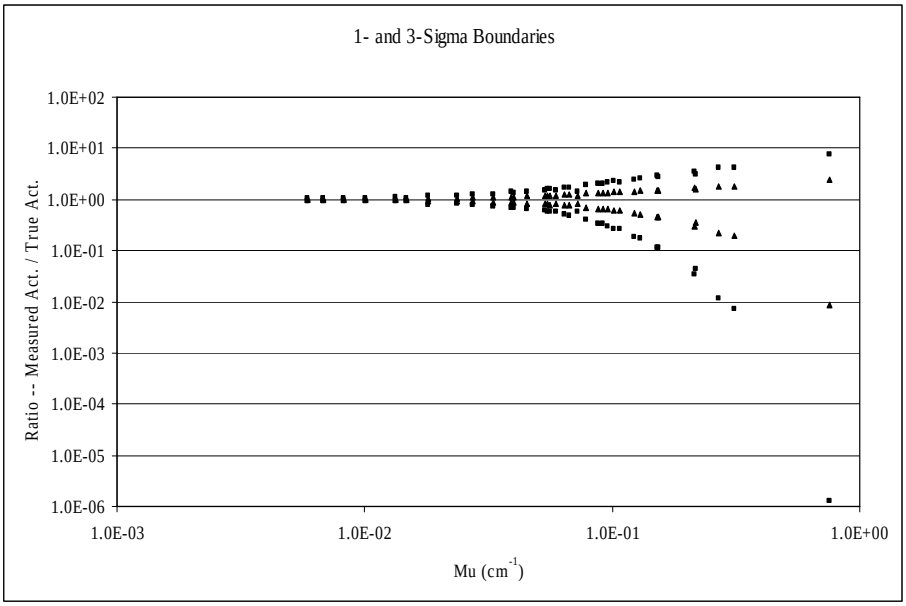

Figure 5. 1- and 3-sigma confidence limits for the 200 liter drum.

Discussion and Conclusions

A Monte Carlo technique had been developed to estimate the quantitative effects of nonuniformities on the results of gamma-ray assays of large containers. The technique represents the gamma-ray detectors as point-like sensors positioned outside the container. The activity in the container is assumed to reside on an operator-definable set of point sources which are randomly positioned throughout the container. For all containers, the distributions of assay results appear to be symmetric and approximately Gaussian-shaped around unity for benign matrices. For more attenuating matrices, the distributions become increasingly asymmetric and skewed towards under-reporting of the true activity. For SLB2 containers, the TMU values to the probabilistic equivalent of $\pm 3\sigma$ bounds can become quite large – on the order of factors of 10 to 100. For smaller containers such as drums, the behavior is similar but less drastic in magnitude. Currently it appears there are too many parameters that effect these distributions – number and location of detectors, container size, etc. – to allow easy quantitative generalization. However, the Monte Carlo technique can be used to quickly estimate these behaviors as input to simpler TMU parameterizations. Future work will report results for a wider range of containers and materials. The calculations will be extended to other assay configurations and the impact of matrix heterogeneity will be included.

References

[1] X-5 Monte Carlo Team, "MCNP – A General Monte Carlo N-Particle Transport Code, Version 5," LANL Publications LA-UR-03-1987, LA-CP-03-0245, and LA-CP-03-0284.

[2] R. Venkataraman, F. Bronson, V. Atrashkevich, B. M. Young, and M. field, "Validation of in situ object counting system (ISOCS) mathematical efficiency calibration software," *Nuclear Instruments and Methods in Physics Research,* A442 (1999) 450.